RESEARCH ARTICLE

Projected changes in drought characteristics over the Western Cape, South Africa

Myra Naik [iD] | Babatunde J. Abiodun [iD]

Department of Environmental and Geographical Science, Climate System Analysis Group, University of Cape Town, Cape Town, South Africa

Correspondence
Myra Naik, Department of Environmental and Geographical Science, Climate System Analysis Group, University of Cape Town, Cape Town, South Africa.
Email: myranaik@gmail.com

Abstract

The devastating socioeconomic impacts of recent droughts in the Western Cape have intensified the quest for future drought mitigation measures. While ongoing global warming may increase atmospheric evaporative demand and worsen drought conditions, most studies on drought in the Western Cape have overlooked the role of potential evapotranspiration (PET). The present study examines the role of PET on future drought characteristics, focusing on four river catchments. Two drought indices, the Standardized Precipitation Index (SPI) and the Standardized Precipitation Evapotranspiration Index (SPEI), were analysed. The capability of the Co-ordinated Regional Downscaling Experiment simulations to reproduce the drought characteristics was evaluated by comparing present-day climate simulations with observations. The impacts of different global warming levels (GWLs) on the SPI and SPEI projections were assessed using self-organizing map (SOM) classifications. The results project that a robust drying signal across the Western Cape, but the magnitudes of the projections, which vary across the river catchments, increase with the GWLs. The changes in the drought intensity and frequency are weaker when using the SPI than the SPEI, suggesting that SPI projections may underestimate the influence of global warming on drought because they do not account for the influence of PET. The SOM classification confirms the differences between the two drought indices reveals the drought patterns that are not seen in the drought ensemble means. Nevertheless, the study underscores the need to mitigate future drought impacts over the Western Cape, but with careful consideration on the drought index used in characterizing the droughts.

KEYWORDS
climate change, drought, evapotranspiration, river catchments, South Africa, Western Cape

1 | INTRODUCTION

The Western Cape recently experienced one of the most severe droughts in its history. The multi-year drought was rare because it manifested across four drought classes: meteorological, agricultural, hydrological and socioeconomic. Characterized by below normal rainfall for three consecutive years (2015–2017), the meteorological drought had a cascading series of impacts. The extreme lack of rainfall compromised agricultural and livestock production in the

Western Cape's farmlands, reduced water levels in the major dams to critically low levels and resulted in severe water restrictions (50 L *per* person *per* day) for citizens and local businesses, as they braced themselves for what the City of Cape Town termed "Day Zero" (the event when the city's domestic taps would run dry) (https://coct.co/water-dashboard). Although similar rainfall deficits have occurred in previous years, the impacts of the recent drought were particularly severe. Indeed, it may be that the severity of the recent drought-induced water crisis was exacerbated by human aspects, including poor management, lack of foresight and increased water demand due to population growth (Bohatch, 2017).

Most research that focused on the meteorological aspects of the drought used only rainfall to estimate drought intensity, overlooking the role of evapotranspiration on drought. Some studies have also shown that climate projections of droughts without including evapotranspiration may underestimate the intensity and severity of future droughts (Abiodun *et al.*, 2018). Thus, evapotranspiration may play a crucial role in quantifying droughts in the Western Cape. A good understanding of how to reduce evapotranspiration across the river catchments of the Western Cape may also be valuable for mitigating the negative impacts of future droughts under global warming, and this is thus the focus of the present study.

In an effort to mitigate future climate change, an international agreement called the Paris Agreement was signed in 2015 under the United Nations Framework Convention on Climate Change. The agreement represents an important milestone in international co-operation, since it aims to limit global warming levels (GWLs) to 1.5, 2.0, 2.5 and 3.0°C. Subsequently, there has been some discussion by the scientific community on how achieving this target may significantly mitigate both global (e.g. Gosling *et al.,* 2017) and regional (e.g. Klutse *et al.,* 2018; Nikulin *et al.,* 2018; Osima *et al.,* 2018) warming. Some studies suggest a significant increase in the occurrence of drought over many regions (e.g. Dai and Zhao, 2017; Lehner *et al.,* 2017). Thus far, there have been no known studies on how these GWL targets may affect drought characteristics (such as frequency and intensity) over the Western Cape (South Africa) in the future. Understanding these impacts is important to inform climate-sensitive decision-making better and to assist policymakers in their efforts to minimize the associated potential impacts.

Many studies have examined the potential impacts of climate change on water resources, but their analyses have focused on a sub-regional or country scale (Kusangaya *et al.,* 2014). For instance, Li *et al.* (2015) found a strong climate change signal over the humid tropical areas of Southern Africa, with some variation in precipitation across different months and sub-regions. However, their study made use of a single hydrological model driven by a regional climate model (RCM) to examine the potential impact of future climate change. Graham *et al.* (2011) explored hydrological responses to climate change over a single river basin (in South Africa) using a downscaled multi-model ensemble. Their study found considerable variability amongst these projections. Whilst future temperatures were shown to increase in all of them, there was no consensus for the impacts on future run-off. Their work highlighted the need for additional, well co-ordinated regional climate downscaling studies in the region to define the range of uncertainties involved. More recently Abiodun *et al.* (2018) examined the projected impacts of global warming on droughts over four major river basins in Southern Africa by analysing the multi-model regional climate simulations from the Co-ordinated Regional Climate Downscaling Experiment (CORDEX). However, while the study focused on drought across Southern Africa, it did not examine climate changes in the Western Cape region in particular. Moreover, decisions on water resources management are usually undertaken at the local level and, as such, there is an urgent need for more research focused at the catchment scale (Kusangaya *et al.,* 2014).

Hence, the aim of the present study was to examine the potential impacts of future droughts over four river catchments of the Western Cape. The CORDEX multi-model ensemble was used to examine the characteristics of drought variables in each catchment area for both present-day and future climates under different GWLs (1.5, 2.0, 2.5 and 3.0°C), and a self-organizing map (SOM) was used to classify the drought patterns. The research findings obtained here may offer an informative template for water management policymakers on the impacts of future droughts in the Western Cape's catchment areas. The paper is structured as follows: Section 2 describes the data and methods used in the study, Section 3 presents the results and discussion and Section 4 gives the conclusions of the study.

2 | METHODOLOGY

2.1 | Study region

The Western Cape Province in South Africa is located in the southernmost part of Southern Africa (Figure 1). The province is bordered by the Northern Cape and the Eastern Cape, as well as the Atlantic Ocean in the west and the Indian Ocean in the south. The climate conditions across the Western Cape are temperate Mediterranean with warm dry summers and mild moist winters. Average summer temperatures range from 15 to 27°C, while winter temperatures range from 5 to 22°C (Hurry and Van Heerden, 1982;
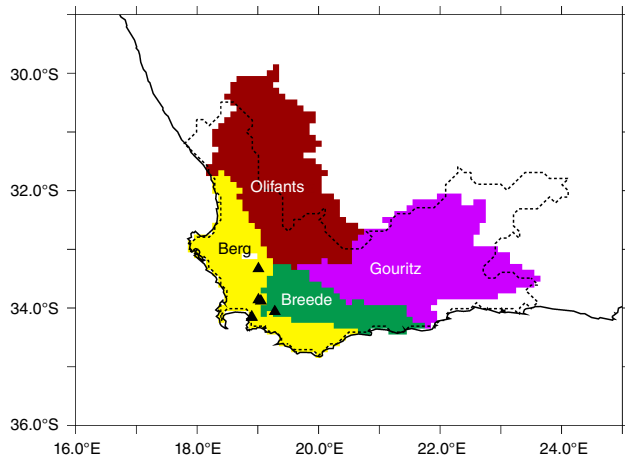
FIGURE 1 The study domain depicting the four main river catchments in the Western Cape region (South Africa). The dashed line delineates the Western Cape Province's political boundary while triangular peaks represent the location of the major dams in that supply region

Tyson, 1986; Kruger, 2004). The Western Cape is one of South Africa's driest regions, receiving only ~350 mm annually, well below the national annual average of ~500 mm (Dennis and Dennis, 2012). Much of the rainfall occurs during the austral winter months (extending from about May to September), typically received from cold fronts and associated extratropical cyclones, or occasional westerly disturbances such as cut-off lows. Rainfall, however, is highly heterogeneous and varies considerably, from semi-arid areas to relatively wet areas on the windward slopes of mountains (Blamey et al., 2017).

Annual precipitation ranges from 300 mm to more than 900 mm, although some areas receive extreme rainfall, i.e. as low as 60 and as high as 3,345 mm (Botai et al., 2017). The present study focuses on the Western Cape's four river systems: the Breede, Berg, Gouritz and the Olifants (Figure 1). The Breede and Berg, which are located entirely within the Western Cape, are arguably the most important of these. Six major dams within these two river catchments form part of the Western Cape Water Supply System. These networks of pump stations and pipelines are key, since they support industry and tourism in the Cape Town metropolitan area and supply drinking and domestic water for use in the City of Cape Town, as well as water for irrigation on surrounding farms (e.g. viticulture and fruit farming under irrigation and rain-fed wheat cultivation) (Statistics South Africa, 2010).

2.2 | Data

Two types of datasets were used for the study: observational data and model simulations. Observational data for this study were obtained from the Climate Research Unit (CRU) and produced by the University of East Anglia (Mitchell and Jones, 2005; Harris et al., 2014). CRU data include monthly observations gridded at a horizontal resolution of $0.5° \times 0.5°$ for the period 1901–2009. Simulation data from the RCMs in CORDEX were used too (Nikulin et al., 2018). They consist of RCM data at a grid spacing of $0.44°$ (approximately 50 km) over the African continent. The simulations are driven by the representative concentration pathway (RCP) 8.5 scenario, which is perhaps the most realistic scenario, given the current trajectory of greenhouse gas emissions. Further information

TABLE 1 Global climate models (GCMs) and the downscaling regional climate models (RCMs) for the simulations used in the study

| GCMs | Period of the global warming levels | | | | Downscaling RCMs |
	1.5°C	2.0°C	2.5°C	3.0°C	
CanESM2[a]	1999–2028	2012–2041	2024–2053	2034–2063	RCA4[5]
CNRM-CM5[b]	2015–2044	2029–2058	2041–2070	2052–2081	RCA4[5], CCLM[2], ALADIN[1]
CSIRO-Mk3[c]	2018–2047	2030–2059	2040–2069	2050–2079	RCA4[5]
EC-EARTH-r1[d]	2003–2032	2021–2050	2035–2064	2046–2075	RACMO[4]
EC-EARTH-r3[e]	2006–2035	2023–2052	2036–2065	2047–2076	HIRHAM[3]
EC-EARTH-r12[f]	2005–2034	2021–2050	2034–2063	2047–2076	RCA4[5], CCLM[2]
GFDL-ESM2M[g]	2020–2049	2037–2066	2052–2081	2066–2095	RCA4[5]
HadGEM2-ES[h]	2010–2039	2023–2052	2033–2062	2042–2071	RCA4[5], CCLM[2], RACMO[4]
IPSL-CM5AMR[i]	2002–2031	2016–2045	2027–2056	2036–2065	RCA4[5]
MIROC5[j]	2019–2048	2034–2063	2047–2076	2058–2087	RCA4[5]
MPI-ESM-LR[k]	2004–2033	2021–2050	2034–2063	2046–2075	RCA4[5], CCLM[2], REMO[6],
NorESM1-M[l]	2019–2048	2034–2063	2047–2076	2059–2088	RCA4[5], WRF[7]

Corresponding 30 year period for various global warming levels (1.5, 2.0, 2.5 and 3.0°C) are indicated. For more detailed information see Déqué et al. (2017). The alphabet letters (a–l) and numbers (1–7) in brackets of the GCMs and RCMs (respectively) are tags to represent the simulations (e.g. a5 represents the CanESM2_RCA4 simulation). (Modified after Abiodun et al., 2018.)

about the 20 simulations for the seven CORDEX RCMs can be found in Table 1 (Déqué *et al.,* 2017). The capabilities of the CORDEX simulations to reproduce the characteristics of drought variables (rainfall, temperature, and Standardized Precipitation Index [SPI] and Standardized Precipitation Evapotranspiration Index [SPEI] drought indices) in each river catchment area during the present-day climate were evaluated by comparing the simulation results with observations. The impacts of climate change were assessed using different GWLs (i.e. 1.5, 2.0, 2.5 and 3.0°C, referred to as GWL 1.5, GWL 2.0, GWL 2.5 and GWL 3.0, respectively) (Nikulin *et al.,* 2018). Note that the time periods for the global climate model (GCM) simulations vary for each GWL period (Table 1).

2.3 | Calculation of drought

Drought over the Western Cape was characterized by using the SPI (McKee *et al.,* 1993) and the SPEI (Vicente-Serrano *et al.,* 2010). Many studies (e.g. Meque and Abiodun, 2015; Ujeneza

and Abiodun, 2015; Araujo *et al.,* 2016) have demonstrated the usefulness of the SPI/SPEI in the Southern African context. The two indices are similar, and both are suitable for calculating drought indices at different time scales. However, while the SPI calculates the drought based on precipitation only, the SPEI represents droughts over an area using the climatic water balance of the area; hence, it calculates drought as the difference between the precipitation and the potential evapotranspiration (PET), i.e. the atmospheric evaporative demand. As the SPEI calculation is based on the water balance, it can be used to identify a drought caused by a decrease in rainfall or higher water demand (i.e. evaporation) or both. Using the CRU observations and the CORDEX data as input for the SPI/SPEI drought algorithms in R statistical software (Vicente-Serrano *et al.,* 2010; Beguería and Vicente-Serrano, 2013), 12 month drought indices (ending in March, which is the end of the rainfall season in the Western Cape) were obtained.

Different methods have been used for calculations of PET, e.g. the Thornthwaite (1948), Hargreaves and Samani
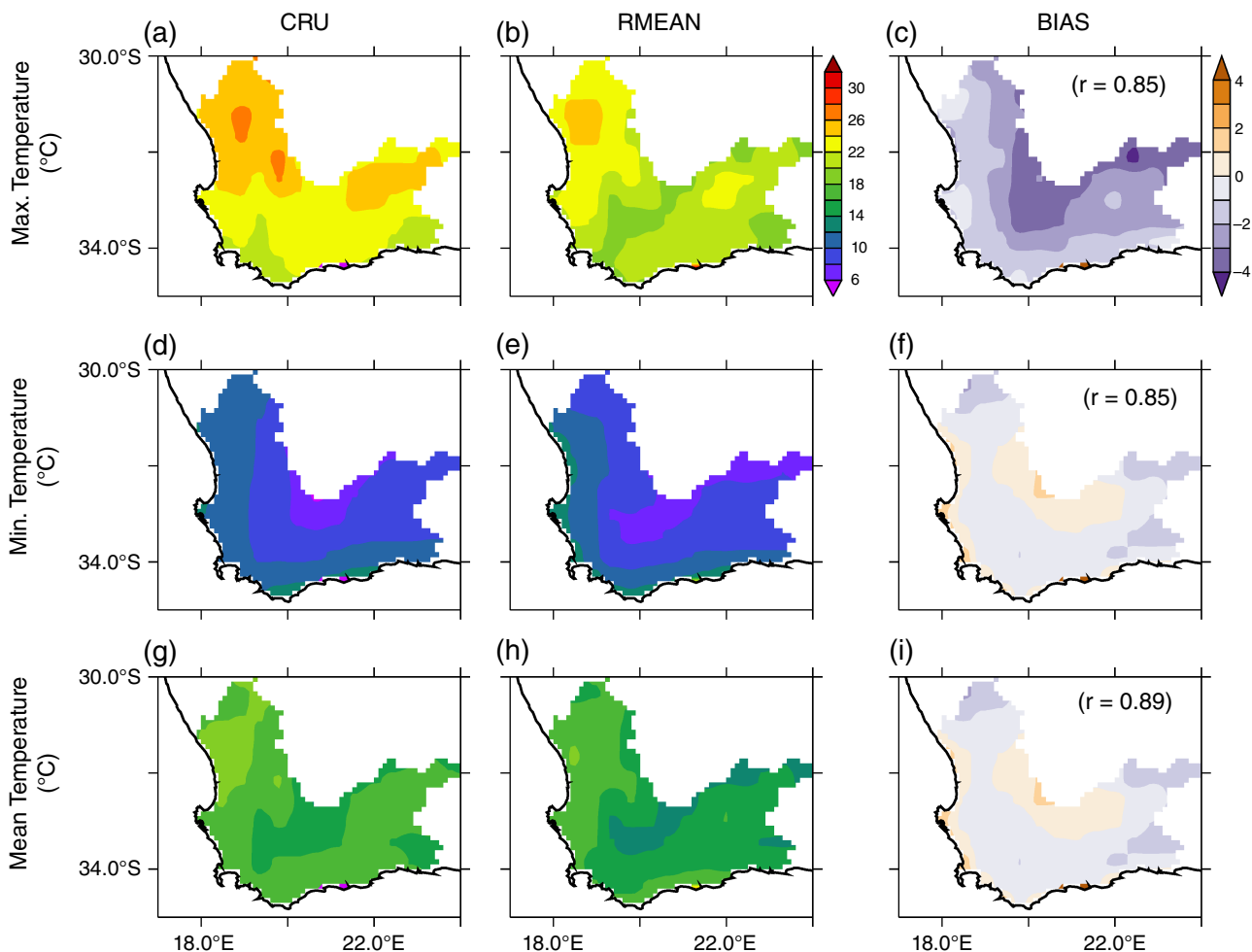

FIGURE 2 The climatology for near-surface maximum, minimum and mean temperatures (°C) over the Western Cape, South Africa (for 1970–2000), as observed by the Climate Research Unit (CRU) and simulated by the Co-ordinated Regional Climate Downscaling Experiment models (RMEAN). The correlation (*r*) and difference (BIAS; regional climate model – CRU) between the observed and simulated variables are indicated

(1985) and Penman–Monteith (Monteith, 1965) methods. While the Penman–Monteith method is often the preferred approach, it requires extensive data, which are not usually available in data-sparse regions such as Africa. Hence, the Hargreaves method is generally recommended if there are insufficient data for the Penman–Monteith method (Hargreaves and Samani, 1985; Abiodun *et al.,* 2018). Since the CORDEX simulation datasets do not have all the variables needed for the Penman–Monteith method, the Hargreaves method was thus used to calculate the PET (see Abiodun *et al.,* 2018). However, the results of our observed PET and the SPEI are compared with those using the Penman–Monteith method.

2.4 | Self-organizing map (SOM)

An SOM analysis was used to classify the drought patterns into groups. The SOM is an artificial neural networks technique for clustering datasets and reducing the dimensionality of a dataset. It consists of many input nodes and fewer output nodes. Data are presented to the input nodes and

processed such that the output nodes are activated according to the weights associated with each incoming link (Agarwal and Skupin, 2008). Neural network training involves setting these weights and is performed in the hidden layer(s). The popular SOM_PAK algorithm (available from Helsinki University of Technology, 1995) was used to make use of an unsupervised neural network with competitive learning with no hidden layers. This means that the input data presented to the network during training do not correspond to known outcomes of classifications (i.e. input–output pairs). Rather, the output nodes compete for the input vectors, and the weights of the input vectors are adjusted according to the weight of the respective input nodes.

In the present study, the SOM technique was used to classify the climate change patterns (drought index and severe drought frequency) associated with drought in the Western Cape, South Africa. The SOM was thus applied on two datasets separately, using a 12 (4 × 3) node classification. The first dataset consists of the projected changes in the drought intensity (i.e. both SPI and SPEI) for all the GWLs and simulations, while the second dataset consists of
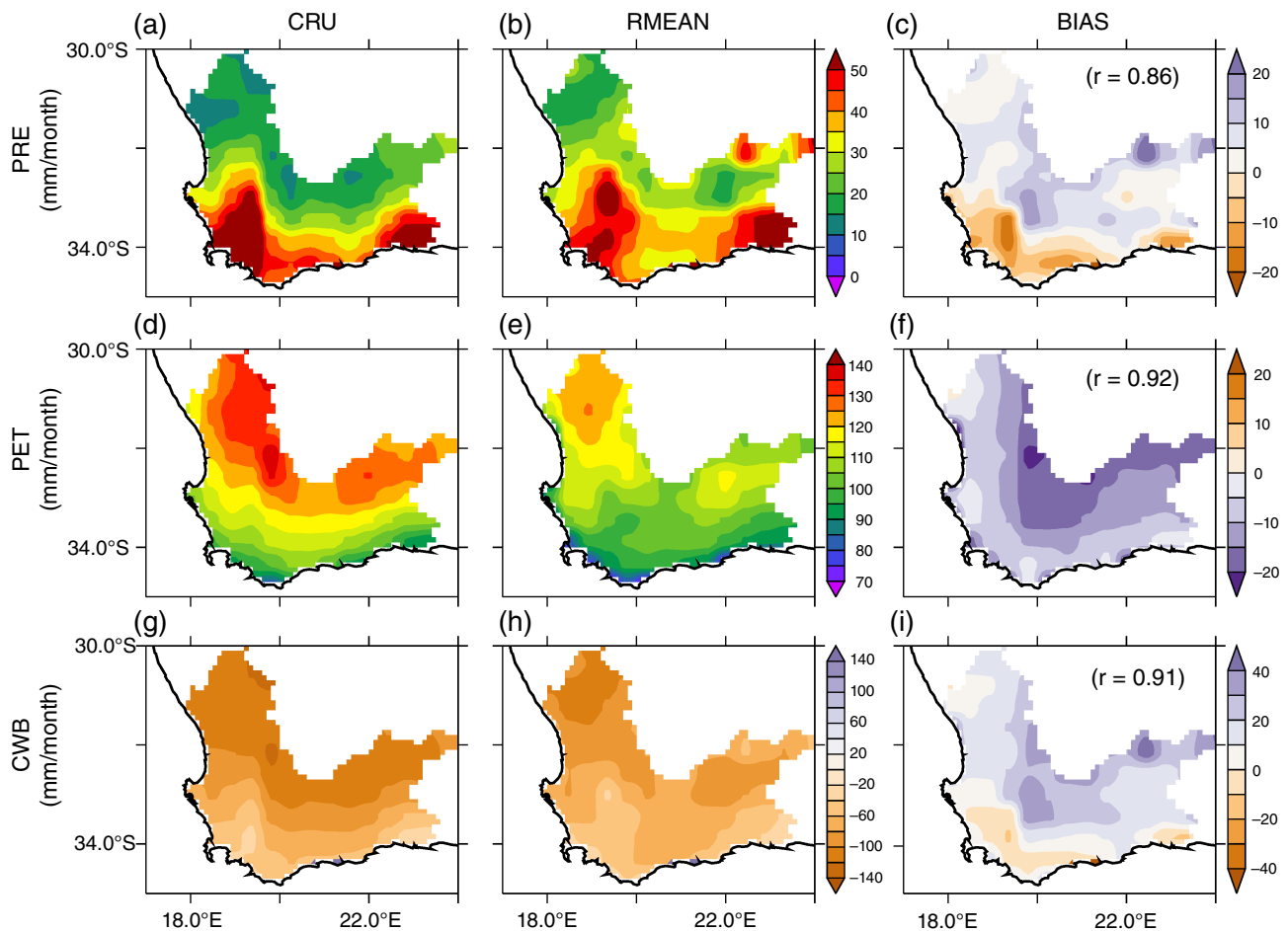

FIGURE 3 As Figure 2 but for moisture variables: precipitation (PRE), potential evapotranspiration (PET) and changes of the climatic water balance (CWB) (CWB = PRE − PET) [Correction added on 25 November 2019, after first online publication: The r values in Figure 3(c) and (i) were previously incorrect and have been updated in this current version.]

the projected changes in the severe drought frequency (i.e. 12-month SPI < −1.5; 12-month SPEI < −1.5). For each dataset, the contribution of each drought index (SPEI and SPI), each GWL, and each simulation to individual SOM node was obtained. Following a previous study by Abiodun *et al*. (2018), the contribution of each drought index, each GWL and each simulation to a SOM node was considered.

3 | RESULTS AND DISCUSSION

3.1 | Climate model evaluation

In this section, the capability of the CORDEX models to simulate the climate in the Western Cape is evaluated. The present-day climate simulation data were compared to observation data to determine how well the models are able to reproduce the temperature and moisture fields and drought over the river catchments.

The models capture the spatial distribution of major climate variables across the Western Cape region. The model ensemble (hereafter, RMEAN) reproduces all the essential climatic features in the observed temperature and moisture fields. For example, it captures the location of the temperature maxima over the West Coast (about 24°C) and of the

temperature minima along the central interior (about 6°C over the Cape Winelands), showing good agreement with the CRU observation data ($r = 0.85$, 0.85 and 0.89 for maximum, minimum and mean temperatures, respectively; Figure 2). The models also reproduce the spatial gradient in the precipitation field and show high correlation with observation ($r = 0.86$). In agreement with CRU data, the models simulate drier conditions (about 15 mm/month) over the West Coast (around 32 ° S, 18 ° E) with increasingly wet conditions (about 50 mm/month) toward the southern Cape Peninsula (between 34 ° S, 18 ° E; Figure 3). Nevertheless, the simulations do feature some biases. For instance, the models underestimate the magnitude of the temperature maxima, producing a cold bias (of about 4°C) over the most part of the Western Cape. A dry bias (about 15 mm/month) also occurs over parts of the Overberg, while a wet bias (about 5 mm/month) occurs further inland over parts of the Cape Winelands and the Central Karoo. It may be that the biases in the simulated rainfall and temperature also produce inherited biases in derived variables, such as PET (of about −20 mm/month) over the Kalahari Basin.

The models also give a credible simulation of the annual cycles of the climate variables over each of the four catchment areas (Figure 4). Over each catchment, the simulation
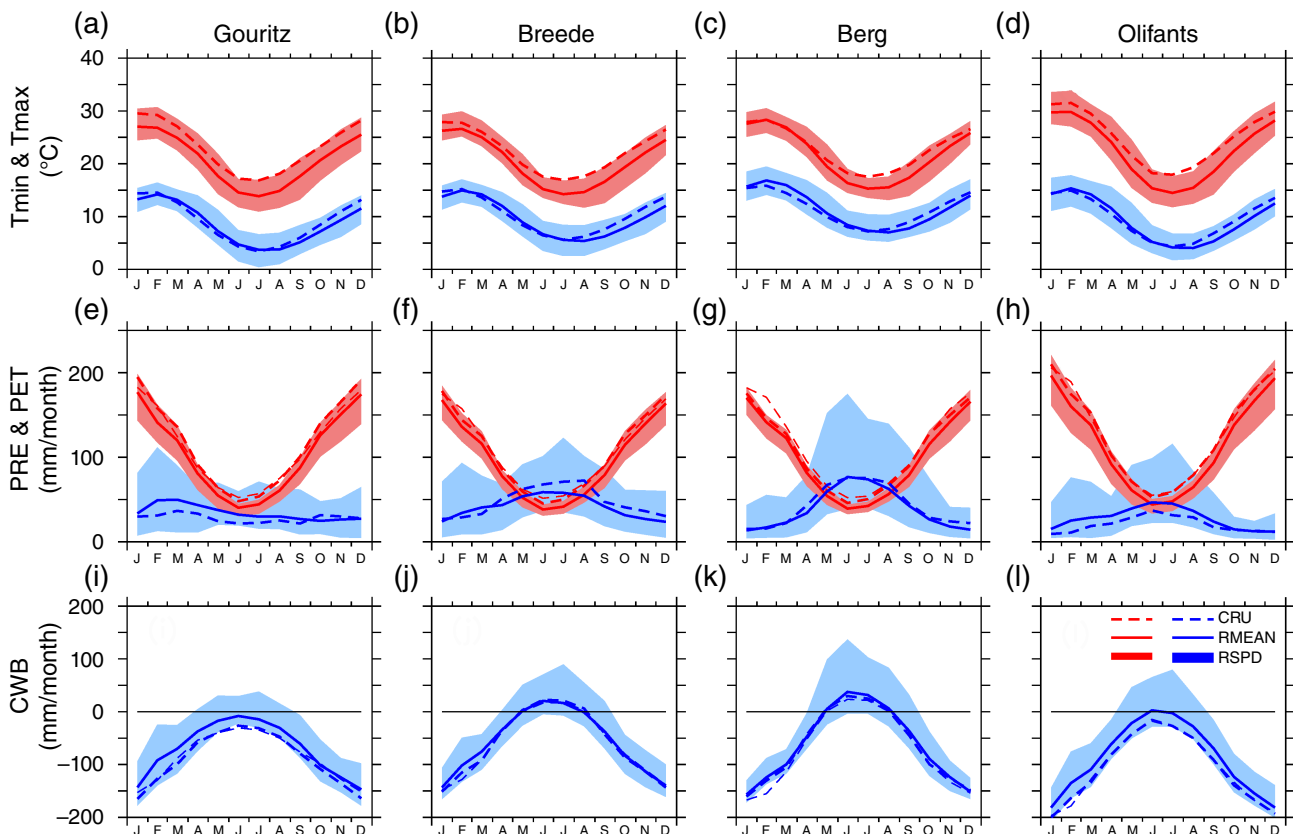

FIGURE 4 The annual cycle of climate variables over the major river catchment in the Western Cape (1970–2000) as observed by the Climate Research Unit and simulated by the Co-ordinated Regional Climate Downscaling Experiment model ensemble (RMEAN)

spread encloses the observation value, and for all the variables RMEAN closely follows the observed annual cycle. The models also capture differences in the annual cycles over the catchments. For instance, in agreement with the observation data, RMEAN shows that, while the Breede, Berg and Olifants River catchments receive their maximum precipitation (about 50, 75 and 45 mm/month, respectively) during the winter months (June to August) and experience dry conditions in the summer, the Gouritz River receives rainfall throughout the year but with a peak (50 mm/month) during the summer months (January to February). This is because the Gouritz River straddles the winter rainfall and summer rainfall regions of the Western Cape region. However, both the observation and the model simulations agree that, despite differences in the annual precipitation cycle, the climate water balance over all the basins reaches its maximum values (−5 to +50 mm/month) during the winter months and its minimum values during the summer months, thus mirroring the PET cycles.

The performance of the models in simulating drought intensity and frequency over the river catchment depends on the index used to characterize the drought (Figure 5). Although the simulated spread in drought frequency resembles the observed spread (Figure 5g), there is better agreement between the observed and simulated drought patterns for the SPEI ($r = 0.38$) than for the SPI ($r = 0.24$). The SPEI also provides a better representation of drought frequency across all four catchments. For instance over the Breede River catchment, the interquartile range of the drought frequency in the simulated SPI (but not the SPEI) overestimates the observed frequency.

3.2 | Projected changes in drought characteristics over the river catchments

The model projections show that the SPEI drought increases across the Western Cape for all GWLs, but the drying patterns are not homogeneous across the region
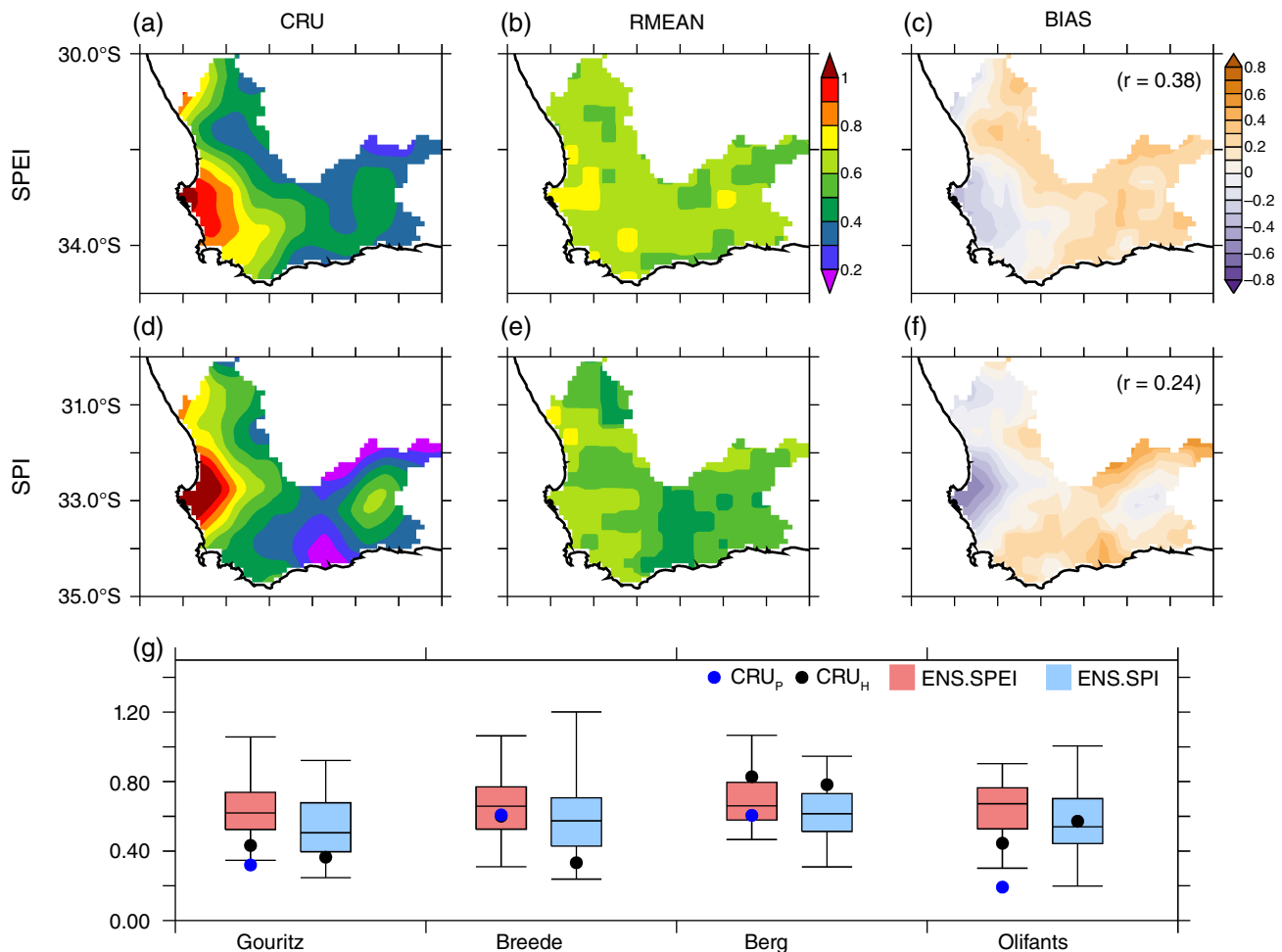

FIGURE 5 The frequency of severe drought (Standardized Precipitation Evapotranspiration Index SPEI ≤ −1.5; Standardized Precipitation Index SPI ≤ −1.5) over the Western Cape (South Africa) (a)–(f) and over each river catchment (g) for the period 1970–2000, as depicted by the Climate Research Unit (CRU) and the Co-ordinated Regional Climate Downscaling Experiment model ensemble simulations

(Figure 6a–d). Projections of the SPEI drought intensity under GWL 1.5 suggest that more intense drying may occur towards the northwestern parts, particularly over the interior of the Olifants River catchment (−1.0). This pattern is similar for higher GWLs (i.e. 2.0, 2.5 and 3.0), except that the intensity of the droughts increases with the GWLs (Figure 6b, c, and d). Projections of severe drought frequency in terms of the SPEI reflect a similar pattern, showing an enhanced occurrence over the northwestern catchments compared to the southeastern catchments for successive GWLs (Figure 6i–l). The peak in SPEI drought frequency across the Olifants River system increases progressively from 2 and 4 events/decade for GWL 1.5 and GWL 2.0 (respectively) to 3 and 5 events/decade for GWL 2.5 and GWL 3.0 (respectively). These results are in line with previous studies on projected circulation changes over the region. For instance, simulations by Engelbrecht *et al.* (2009) also suggest a displacement of frontal rain-bands south of the Southern African subcontinent due to an increase in the intensity and frequency of upper-level high

pressure systems. Such changes would decrease projected rainfall over the region, which may contribute to drier conditions over the Western Cape catchments in the future, as found in the present study.

The model projections using the SPI also show that drought may increase across the region, although the intensity and the spatial distribution differ from that of SPEI (Figure 6e–h). Projections of SPI drought intensity show homogeneous drying (−0.4) for GWL 1.5 (Figure 6e) and a pattern of increased drying over the northwestern areas (about −1.0) compared to parts of the southeastern catchments (−0.4) for the remaining GWLs. Yet the maximum drying for the SPI under GWL 3.0 does not exceed that of the SPEI under GWL 1.5 (Figure 6h and a, respectively). Similarly, projections of severe drought frequency using the SPI are lower than those obtained using the SPEI, and they extend across a smaller spatial area. For instance, under GWL 3.0, the severe drought frequency maxima in terms of the SPI are limited to the Berg River catchment (two droughts/decade; Figure 6h). In contrast, when using the
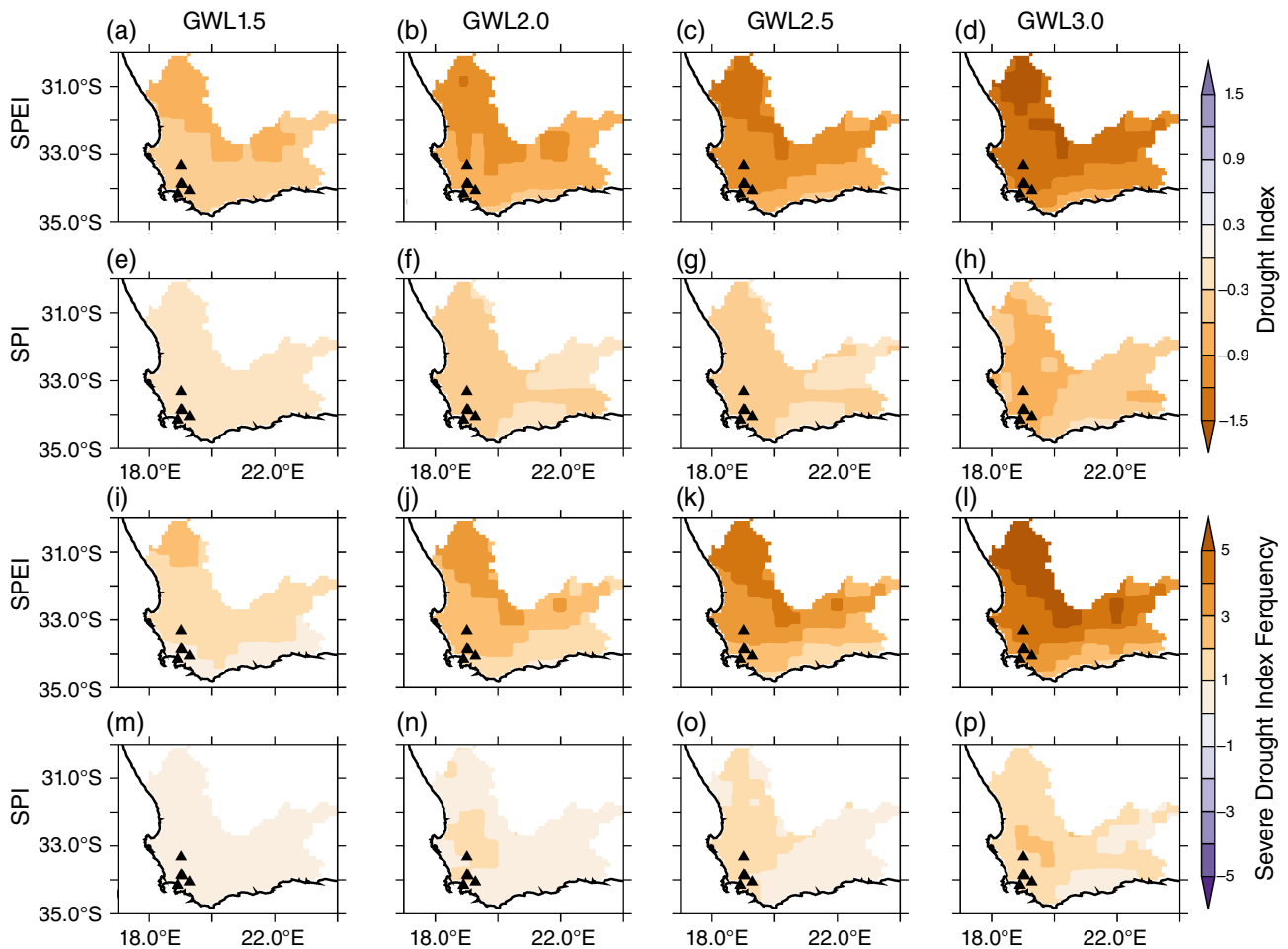

FIGURE 6 Projected changes in drought index (for the Standardized Precipitation Evapotranspiration Index SPEI and the Standardized Precipitation Index SPI) (a)–(h) and severe drought frequency (for SPEI and SPI) (i)–(p) for different global warming levels (GWLs) (GWL 1.5, GWL 2.0, GWL 2.5 and GWL 3.0) over the Western Cape (South Africa)
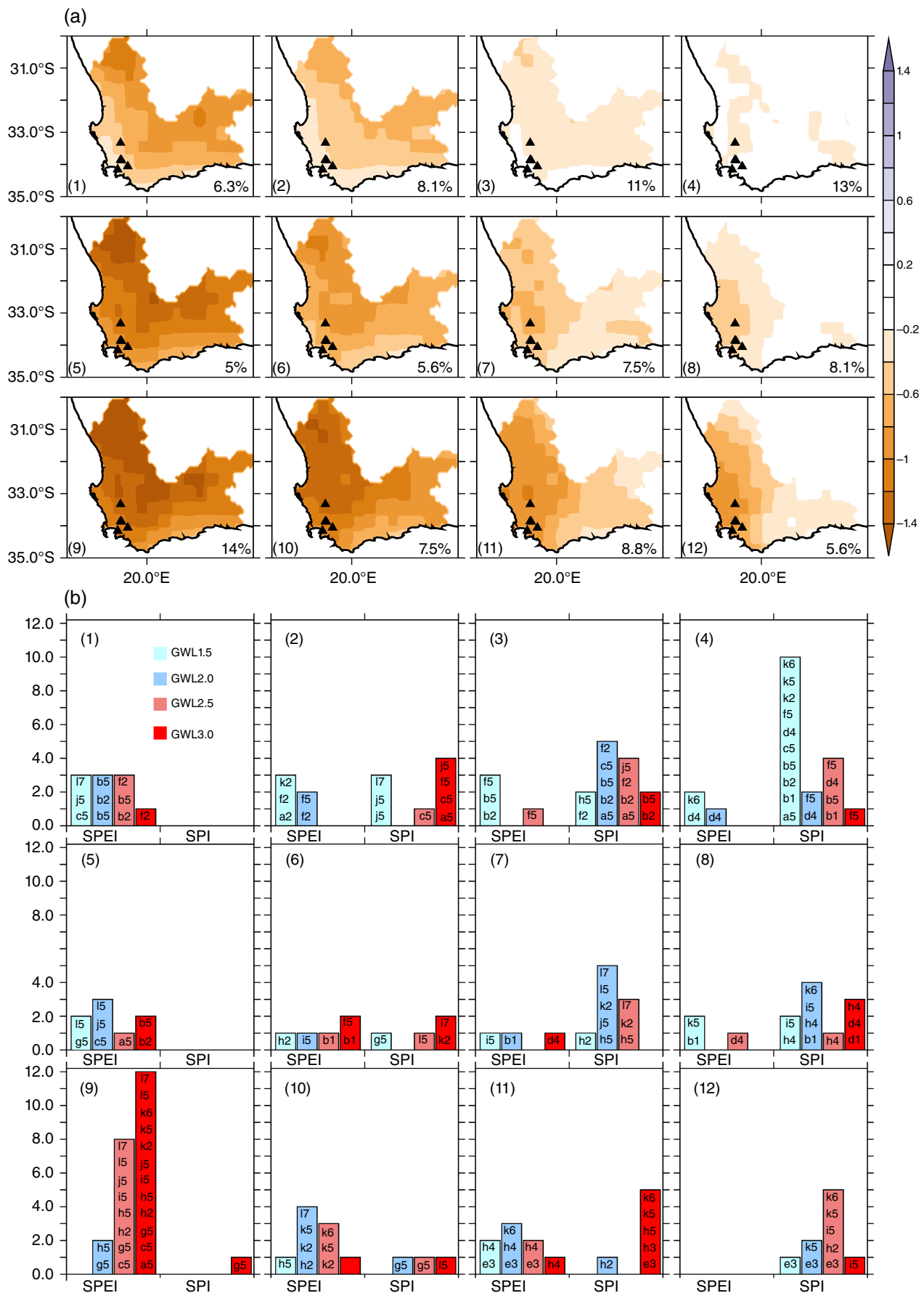
FIGURE 7   Legend on next page.

SPEI, these maxima extend across the Olifants River and are greatly enhanced (more than five droughts/decade; Figure 6d). These findings compare well to those of a previous study by Botai *et al.* (2017), which found a similar spatial contrast between parts of the Western Cape, where the southern and western parts experienced more frequent, more intense and more severe droughts than the eastern parts of the Province. Similarly, Oguntunde *et al.* (2006) found an increase in drought intensity and spatial extent for the SPEI and SPI over the Volta River Basin (West Africa), where the magnitude of the increase was higher with the SPEI than with the SPI.

The SOM classification of the simulated severe drought intensity over the Western Cape region shows four extreme patterns. Each pattern is located near the edges of the SOM (Figure 7a) and is linked to differences between the drought indices (Figure 7b). In the first pattern (i.e. nodes 1, 2, 5 and 6), the drying peaks over the northern parts of the Olifants and the central Gouritz River catchments. The four nodes associated with the first pattern contribute a high percentage of the variability in drought intensity (25%). Model simulations contributing to this node are better explained by drought intensity using the SPEI (rather than the SPI). These drought patterns (especially nodes 1 and 5) are dominated by SPEI projections (Figure 7).

The second pattern (i.e. nodes 9 and 10) is characterized by severe drought (about $-1.5°C$) especially over the northern parts of the Olifants River catchment (Figure 7). The two nodes associated with this pattern also contribute to variability in drought intensity (about 22%). The second pattern, best represented by node 9, is comparable spatially to the SPEI model ensemble mean (Figure 6d). Model simulations contributing to this node are also better explained by drought intensity in terms of the SPEI (rather than the SPI). The number of simulations that project node 9 patterns for SPEI drought increases as the the GWL increase. While no simulation projects it at GWL1.5, two simulations project at GWL2.0, eight at GWL2.5 and twelve at GWL3.0.

In the third pattern (i.e. nodes 3, 4, 7 and 8), drought is not severe over much of the region. Nodes associated with the third pattern account for the largest percentage of the SOM variability in drought intensity (about 40%). The third pattern is well represented by node 4, which shows a weak drying signal across all four catchments. Model simulations for this node are better represented by SPI drought (Figure 6e-h).

Note that the number of simulations showing this pattern for drought severity decreases for higher GWLs (Figure 7b). For instance, with SPI, while ten simulations feature it at GWL1.5, only one simulation suggest it at GWL3.0.

The fourth pattern (i.e. nodes 7, 8, 11 and 12) shows a west–east spatial gradient in drought intensity. The pattern, which accounts for 30% of the projected drought, compares more to the SPI ensemble mean than the SPEI (Fig compare 6 and 7). It is well represented by node 12, which shows a peak drought intensity over the central Berg River catchment (about -1) and a relative decrease towards the Breede River (about -0.5). The results of the SOM classification for simulated drought frequency are similar to that of drought intensity, although there are some differences in the number of simulations showing the respective pattern for drought frequency at higher GWLs (Figure 8a,b).

There is a robust drying signal across the Western Cape because the models show good agreement with regard to the various river catchments; this agreement varies, depending on the GWL and the drought index used (Figure 9). In most cases, at least 75% of the models agree on the drying signal. For example, across successive GWLs, the models show an increase in drought intensity and frequency over all the catchments. Over the Olifants River, for example, the model ensemble shows that drought intensity increases across successive GWLs, both for the SPI (from -0.1 to -1.0) and for the SPEI (about -0.5 to -2.0) (Figure 9d). The model ensemble further shows that drought frequency increases across successive GWLs, both for the SPI (from 0.1 to 2 events/decade) and for the SPEI (from 0.1 to 4 events/decade; Figure 9h). This pattern in the drying signal varies over the other three catchments, with some differences in the model spread. The model ensemble for drought in the Breede River catchment using the SPEI is less severe than in the Olifants River, for both drought intensity (-0.1 to -1.1; Figure 9b) and frequency (from 0.1 to 3.5 events/decade; Figure 9f). Additionally, the degree of drying also varies depending on the drought index used. The SPI projects a lower value than the SPEI for drought. For instance, over the Olifants River, for GWL 3.0 (RCP8.5), the ensemble mean for SPI drought intensity (-0.5) is less than that of the SPEI (-2.0), and the SPI drought frequency (0.5) is also less than that of the SPEI (7.0). The reason for this may be that, since the SPI does not incorporate PET, it may underestimate the drought.

FIGURE 7 (a) Self-organizing map distribution (3 × 4 nodes) of projections for drought (Standardized Precipitation Index SPI and Standardized Precipitation Evapotranspiration Index SPEI) patterns over the Western Cape (South Africa) for different global warming levels (GWLs) (GWL 1.5, GWL 2.0, GWL 2.5 and GWL 3.0). The numbers at the lower left and lower right corners of each node represent the tag and percentage contribution of each pattern, respectively. (b) The frequency of the patterns under each GWL, drought index and simulation. The codes in each bar are the tags of the simulations making up the bar. In a simulation tag, an alphabet letter indicates the global climate model while the number denotes the regional climate model (e.g. a5 represents the CanESM2_RCA4 simulation); see Table 1
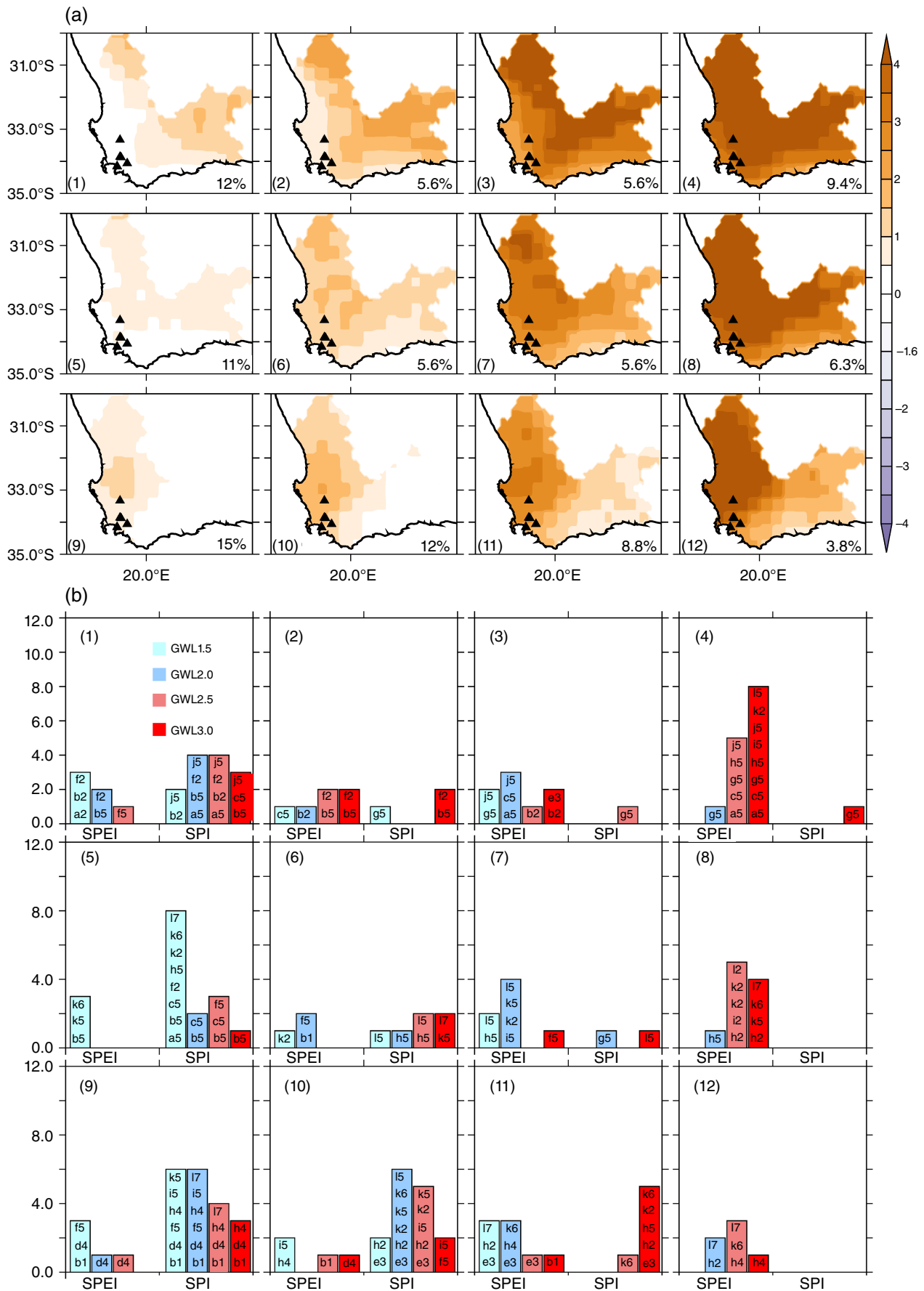
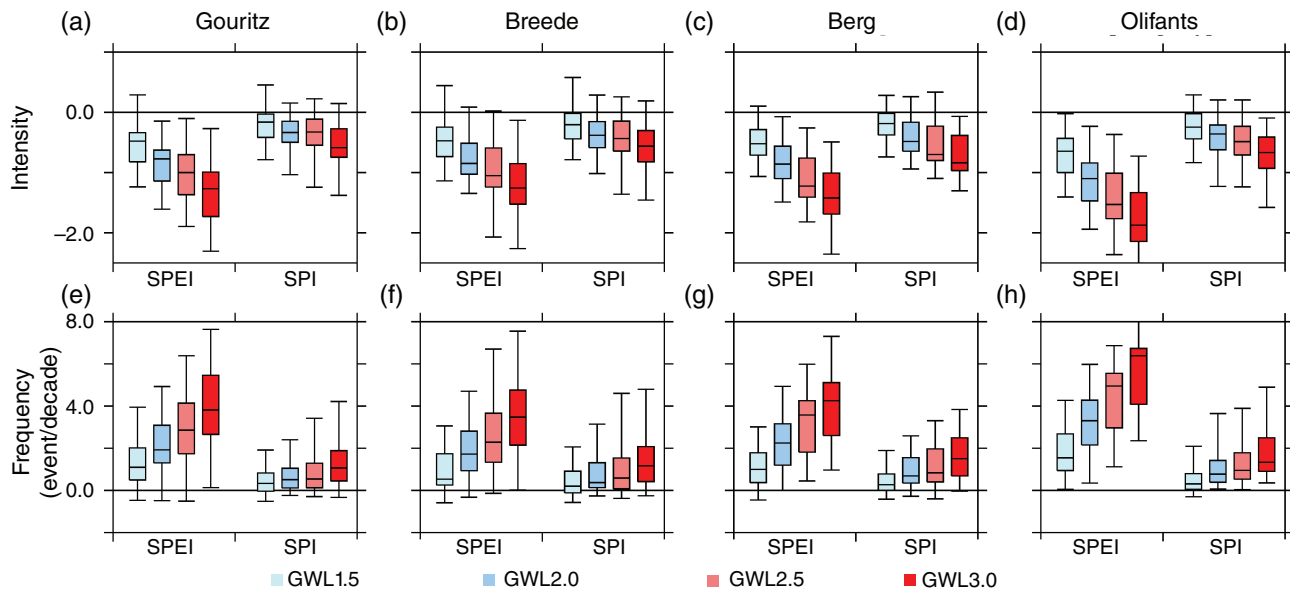**FIGURE 8**   As Figure 7 but for drought frequency

FIGURE 9 Projections of the Standardized Precipitation Evapotranspiration Index (SPEI) and the Standardized Precipitation Index (SPI) severe drought intensity (a)–(d) and frequency (e)–(h) over the four river catchments in the Western Cape (South Africa)

These findings have some implications for water resource managers operating in the Western Cape river catchments. There is good model agreement on the sign of change across the region. The robust drying signal projected for the future across the entire Province underscores the need for developing a mitigation strategy to reduce drought impacts. Additionally, it may also be necessary carefully to consider the drought index used when developing such a strategy. Depending on the drought index used, projections may indicate higher or lower values of drought impacts, thereby either overestimating or underestimating the influence of global warming on drought. As illustrated above, the SPI and SPEI drought indices produce considerable differences in the model ensemble spread. The study furthermore highlights the role of PET as a key variable, in both drought monitoring and prediction over the region, and potentially in mitigating the harmful impacts of droughts and water scarcity across the Western Cape in the future.

4 | CONCLUSION

In this study, Co-ordinated Regional Climate Downscaling Experiment (CORDEX) data were used to examine the potential impacts of various global warming levels (GWLs) (1.5, 2.0, 2.5, 3.0°C) on future drought in four river catchments across the Western Cape. The Standardized Precipitation Index (SPI) and the Standardized Precipitation Evapotranspiration Index (SPEI) were used to quantify drought (in terms of frequency and intensity), and a self-organizing map was also used to classify the different

drought patterns. The present-day climate (1971–2000) simulations were compared with observations in order to evaluate the capability of the CORDEX simulations to reproduce the characteristics of drought variables over the region accurately; thereafter, the projected changes in future droughts were examined. The results of the study suggest the following.

- The CORDEX models correctly capture the spatial distribution of major climate variables over the Western Cape region and reproduce the essential climatic features in the observed temperature and moisture fields.
- The models also give a credible simulation of the annual cycles of the climate variables over each of the four catchments. However, the accuracy of the model's performance in simulating the drought intensity and frequency over the river catchments depends on the index used in characterizing the drought.
- Projected changes in drought characteristics over the river catchments show a robust drying signal, but this varies depending on the GWL, the river catchment and the drought index used.
- When using the SPEI, drought increases across the Western Cape for all GWLs, although the drying pattern is not homogeneous across the region. When using the SPI, drought may also increase over the region but the intensity and the spatial distribution are different.

This study highlighted the role of potential evapotranspiration (PET) as a key variable in characterizing drought in the Western Cape. It showed that droughts may be more

severe and more frequent in the future under different GWLs. The research underscores the need for developing an effective mitigation strategy to reduce drought impacts, with careful consideration of the drought index being used. Future studies might make use of alternative drought indices (for comparison) or translate these future climate change drought projections to hydrological drought impacts in selected river catchments. Further analysis may also be useful to assess the potential for the mitigation of PET through land use and land cover changes. Such studies would better inform water policymakers in efforts to create sustainable and effective drought adaptation efforts. All these findings have significant implications for water resource managers operating in Western Cape catchment areas.

ACKNOWLEDGEMENTS

ORCID

Myra Naik https://orcid.org/0000-0001-6847-4913
Babatunde J. Abiodun https://orcid.org/0000-0002-3878-0116

REFERENCES

Abiodun, B.J., Nokwethaba, N., Petja, B., Abatan, A.A. and Oguntunde, P.G. (2018) Future projection of droughts over major river basins in Southern Africa at specific global warming levels. *Theoretical and Applied Climatology*, 1–15. https://doi.org/10.1007/s00704-018-2693-0.

Agarwal, P., and Skupin, A. (2008) *Self-organising maps: Applications in geographic information science*. Chichester, England: John Wiley & Sons.

Araujo, J., Abiodun, B.J. and Crespo, O. (2016) Impacts of drought on grape yields in Western Cape, South Africa. *Theoretical and Applied Climatology*, 123, 117–130. https://doi.org/10.1007/s00704-014-13.

Beguería, S. and Vicente-Serrano, S.M. (2013) SPEI: calculation of the standardised precipitation-evapotranspiration index. R Package, version 1, p. 6.

Blamey, R.C., Ramos, A.M., Trigo, R.M., Tomé, R. and Reason, C.J.C. (2017) The influence of atmospheric rivers over the South Atlantic on winter rainfall in South Africa. *Journal of Hydrometeorology*, 19, 127–142.

Bohatch, T. (2017) *What's Causing Cape Town's Water Crisis?*. What's Causing Cape Town's Water Crisis. Available at: https://www.groundup.org.za/article/whats-causing-cape-towns-water-crisis/ [Accessed 16th May 2017].

Botai, C.M., Botai, J.O., de Wit, J.P., Ncongwane, K.P. and Adeola, A.M. (2017) Drought characteristics over the Western Cape Province, South Africa. *Water*, 9, 876.

Dai, A. and Zhao, T. (2017) Uncertainties in historical changes and future projections of drought. Part I: Estimates of historical drought changes. *Climatic Change*, 144, 519–533.

Dennis, I. and Dennis, R. (2012) Climate change vulnerability index for South African aquifers. *Water SA*, 38, 417–426.

Déqué, M., Calmanti, S., Christensen, O.B., Dell Aquila, A., Maule, C.F., Haensler, A., Nikulin, G. and Teichmann, C. (2017) A multi-model climate response over tropical Africa at +2°C. *Climate Services*, 7, 87–95.

Engelbrecht, F.A., McGregor, J.L. and Engelbrecht, C.J. (2009) Dynamics of the Conformal-Cubic Atmospheric Model projected climate-change signal over southern Africa. *International Journal of Climatology: A Journal of the Royal Meteorological Society*, 29, 1013–1033.

Gosling, S.N., Zaherpour, J., Mount, N.J., Hattermann, F.F., Dankers, R., Arheimer, B., Breuer, L., Ding, J., Haddeland, I. and Kumar, R. (2017) A comparison of changes in river runoff from multiple global and catchment-scale hydrological models under global warming scenarios of 1°C, 2°C and 3°C. *Climatic Change*, 141, 577–595.

Graham, L., Andersson, L., Horan, M., Kunz, R., Lumsden, T., Schulze, R., Warburton Toucher, M., Wilk, J. and Yang, W. (2011) Using multiple climate projections for assessing hydrological response to climate change in the Thukela River Basin, South Africa. *Physics and Chemistry of the Earth* (Parts A/B/C), 36 (14–15), 727–735.

Hargreaves, G.H. and Samani, Z.A. (1985) Reference crop evapotranspiration from temperature. *Applied Engineering in Agriculture*, 1, 96–99.

Harris, I., Jones, P.D., Osborn, T.J. and Lister, D.H. (2014) Updated high-resolution grids of monthly climatic observations – the CRU TS3.10 dataset. *International Journal of Climatology*, 34, 623–642.

Helsinki University of Technology. (1995). SOM_PAK algorithms.

Hurry, L. and Van Heerden, J. (1982) *Southern Africa's Weather Patterns: A Guide to the Interpretation of Synoptic Maps*. Goodwood: Via Afrika.

Klutse, N.A.B., Ajayi, V.O., Gbobaniyi, E.O., Egbebiyi, T.S., Kouadio, K., Nkrumah, F., Quagraine, K.A., Olusegun, C., Diasso, U. and Abiodun, B.J. (2018) Potential impact of 1.5°C and 2°C global warming on consecutive dry and wet days over West Africa. *Environmental Research Letters*, 13, 55013.

Kruger, A.C. (2004) *Climate of South Africa: Climate Controls*. Pretoria: South African Weather Service.

Kusangaya, S., Warburton, M.L., Archer van Garderen, E. and Jewitt, G.P.W. (2014) Impacts of climate change on water resources in southern Africa: a review. *Physics and Chemistry of the Earth, Parts A/B/C*, 67-69, 47–54.

Lehner, F., Coats, S., Stocker, T.F., Pendergrass, A.G., Sanderson, B.M., Raible, C.C. and Smerdon, J.E. (2017) Projected drought risk in 1.5°C and 2°C warmer climates. *Geophysical Research Letters*, 44, 7419–7428.

Li, L., Diallo, I., Xu, C.-Y. and Stordal, F. (2015) Hydrological projections under climate change in the near future by RegCM4 in Southern Africa using a large-scale hydrological model. *Journal of Hydrology*, 528, 1–16.

McKee, T.B., Doesken, N.J. and Kleist, J. (1993) The relationship of drought frequency and duration to time scales. In: *Proceedings of the 8th Conference on Applied Climatology*. Boston, MA: American Meteorological Society, pp. 179–183.

Meque, A. and Abiodun, B. (2015) Simulating the link between ENSO and summer drought in Southern Africa using regional climate models. *Climate Dynamics : Observational, Theoretical and Computational Research on the Climate System*, 44(7–8), 1881–1900.

Mitchell, T.D. and Jones, P.D. (2005) An improved method of constructing a database of monthly climate observations and associated high-resolution grids. *International Journal of Climatology*, 25, 693–712.

Monteith, J.L. (1965) Evaporation and environment. In: The state and movement of water in living organisms. *XIXth Symposium of the Society Experimental Biology*. New York: Academic Press, p. 205.

Nikulin, G., Lennard, C., Dosio, A., Kjellström, E., Chen, Y., Hänsler, A., Kupiainen, M., Laprise, R., Mariotti, L. and Maule, C. F. (2018) The effects of 1.5 and 2 degrees of global warming on Africa in the CORDEX ensemble. *Environmental Research Letters*, 13, 65003.

Oguntunde, P.G., Friesen, J., van de Giesen, N. and Savenije, H.H.G. (2006) Hydroclimatology of the Volta River basin in West Africa: trends and variability from 1901 to 2002. *Physics and Chemistry of the Earth, Parts A/B/C*, 31, 1180–1188.

Osima, S., Indasi, V.S., Zaroug, M., Seid, E.H., Gudoshava, M., Misiani, H.O., Nimusiima, A., Anyah, R.O., Otieno, G., Ogwang, B.A., Jain, S., Kondowe, A.L., Mwangi, E., Lennard, C., Nikulin, G. and Dosio, A. (2018) Projected climate over the Greater Horn of Africa under 1.5°C and 2°C global warming. *Environmental Research Letters*, 13, 65004.

Statistics South Africa. (2010) *Water Management Areas in South Africa, National Accounts: Environmental Economic Accounts*. Pretoria: Statistics South Africa.

Thornthwaite, C.W. (1948) An approach toward a rational classification of climate. *Geographical Review*, 38, 55–94.

Tyson, P.D. (1986) *Climatic Change and Variability in Southern Africa*. Cape Town, Republic of South Africa: Oxford University Press.

Ujeneza, E. and Abiodun, B. (2015) Drought regimes in Southern Africa and how well GCMs simulate them. *Climate Dynamics*, 4 (5–6), 1595–1609.

Vicente-Serrano, S.M., Beguería, S. and López-Moreno, J.I. (2010) A multiscalar drought index sensitive to global warming: the standardized precipitation evapotranspiration index. *Journal of Climate*, 23, 1696–1718.

How to cite this article: Naik M, Abiodun BJ. Projected changes in drought characteristics over the Western Cape, South Africa. *Meteorol Appl.* 2020;27: e1802. https://doi.org/10.1002/met.1802